NASA-TM-112531

IN-39-TM

Reprinted from

theoretical and applied fracture mechanics

fracture mechanics technology

Theoretical and Applied Fracture Mechanics 25 (1996) 211-224

Computational simulation of damage progression of composite thin shells subjected to mechanical loads

P.K. Gotsis [a,*], C.C. Chamis [a], L. Minnetyan [b]

[a] *Structures Division, National Aeronautics and Space Administration Lewis Research Center, Cleveland, 44135 OH, USA*

[b] *Department of Civil and Environmental Engineering, Clarkson University, Potsdam, 13699 NY, USA*

ELSEVIER

THEORETICAL AND APPLIED FRACTURE MECHANICS

Editor-in-Chief
G.C. Sih, *Institute of Fracture and Solid Mechanics, Lehigh University, Bethlehem, PA 18015, USA*

Board of Editors
Fracture Mechanics Technology
J.T. Barnby, *UK*
C.M. Branco, *Portugal*
A. Carpinteri, *Italy*
A.A. Chamis, *USA*
C.I. Chang, *USA*
S.C. Chou, *USA*
D. Corderoy, *Australia*
A. DiTommaso, *Italy*
M. Elices, *Spain*
K.F. Fischer, *Germany*
K. Friedrich, *Germany*
G.G. Garrett, *South Africa*
E.E. Gdoutos, *Greece*
F. Gillemot, *Hungary*
D.P.H. Hasselman, *USA*
A.R. Ingraffea, *USA*
R. Jones, *Australia*
H.-W. Liu, *USA*
S.N. Monteiro, *Brazil*
O. Orringer, *USA*
C.W. Smith, *USA*

Mechanics and Physics of Fracture
G.I. Barenblatt, *Russia*
G. Caglioti, *Italy*
E. Kröner, *Germany*
S.T. Mileiko, *Russia*
H. Mughrabi, *Germany*
J.T. Pindera, *Canada*
J.W. Provan, *Canada*
E. Sommer, *Germany*
M. Sokolowski, *Poland*
V. Tamuzs, *Latvia*

© 1996, Elsevier Science B.V. All rights reserved.

No part of this publication may be reproduced, stored in a retrieval system or transmitted in any form or by any means, electronic, mechanical, photocopying, recording or otherwise, without the prior permission of the publisher, Copyright & Permissions Department, Elsevier Science B.V., P.O. Box 521, 1000 AM Amsterdam, The Netherlands.
Special regulations for authors – Upon acceptance of an article by the journal, the author(s) will be asked to transfer copyright of the article to the publisher. This transfer will ensure the widest possible dissemination of information.
Special regulations for readers in the U.S.A. – This journal has been registered with the Copyright Clearance Center, Inc. Consent is given for copying of articles for personal or internal use, or for the personal use of specific clients. This consent is given on the condition that the copier pays through the Center the per-copy fee stated in the code on the first page of each article for copying beyond that permitted by Sections 107 or 108 of the U.S. Copyright Law. The appropriate fee should be forwarded with a copy of the first page of the article to the Copyright Clearance Center, Inc., 222 Rosewood Drive, Danvers, MA 01923, U.S.A. If no code appears in an article, the author has not given broad consent to copy and permission to copy must be obtained directly from the author. The fee indicated on the first page of an article in this issue will apply retroactively to all articles published in the journal, regardless of the year of publication. This consent does not extend to other kinds of copying, such as for general distribution, resale, advertising and promotion purpose, or for creating new collective works. Special written permission must be obtained from the publisher for such copying.

USA mailing notice – Theoretical and Applied Fracture Mechanics (ISSN 0167-8442) is published six times per year by Elsevier Science B.V., Molenwerf 1, P.O. Box 211, 1000 AE Amsterdam, The Netherlands. The annual subscription price in the USA is US$ 585 (valid in North, Central and South America only), including air speed delivery. Periodicals postage is paid at Jamaica, NY 11431.
USA POSTMASTERS: Send address changes to Theoretical and Applied Fracture Mechanics, Publications Expediting, Inc., 200 Meacham Avenue, Elmont, NY 11003. Airfreight and mailing in the USA by Publications Expediting.

No responsibility is assumed by the Publisher for any injury and/or damage to persons or property as a matter or products liability, negligence or otherwise, or from any use or operation of any methods, products, instructions or ideas contained in the material herein.
Although all advertising material is expected to conform to ethical standards, inclusion in this publication does not constitute a guarantee or endorsement of the quality or value of such product or of the claims made of it by its manufacturer.

∞ The paper used in this publication meets the requirements of ANSI/NISO Z39.48-1992 (Permanence of Paper).

ELSEVIER

Theoretical and Applied Fracture Mechanics 25 (1996) 211–224

theoretical and applied fracture mechanics

Computational simulation of damage progression of composite thin shells subjected to mechanical loads

P.K. Gotsis [a,*], C.C. Chamis [a], L. Minnetyan [b]

[a] *Structures Division, National Aeronautics and Space Administration Lewis Research Center, Cleveland, 44135 OH, USA*
[b] *Department of Civil and Environmental Engineering, Clarkson University, Potsdam, 13699 NY, USA*

Abstract

Defect-free and defected composite thin shells with ply orientation $(90/0/\pm 75)$ made of graphite/epoxy are simulated for damage progression and fracture due to internal pressure and axial loading. The thin shells have a cylindrical geometry with one end fixed and the other free. The applied load consists of an internal pressure in conjunction with an axial load at the free end, the cure temperature was 177°C (350°F) and the operational temperature was 21°C (70°F). The residual stresses due to the processing are taken into account. Shells with defect and without defects were examined by using CODSTRAN an integrated computer code that couples composite mechanics, finite element and account for all possible failure modes inherent in composites. CODSTRAN traces damage initiation, growth, accumulation, damage propagation and the final fracture of the structure. The results show that damage initiation started with matrix failure while damage/fracture progression occurred due to additional matrix failure and fiber fracture. The burst pressure of the $(90/0/\pm 75)$ defected shell was 0.092% of that of the free defect. Finally the results of the damage progression of the $(90/0/\pm 75)$, defective composite shell was compared with the $(90/0/\pm\theta)$, where $\theta = 45$ and 60, layup configurations. It was shown that the examined laminate $(90/0/\pm 75)$ has the least damage tolerant of the two compared defective shells with the $(90/0/\pm\theta)$, $\theta = 45$ and 60 laminates.

1. Introduction

Aircraft, marine and automotive vehicle industries use composite shells because of their low weight and high stiffness and stability features. Design considerations with regard to the durability of composite shells require a priori evaluation of damage initiation and propagation mechanisms under expected service loads. Concerns for safety and survivability of critical components require quantification of the composite structural damage tolerance during overloads. Characteristic flexibilities in the tailoring of composite structures make them more versatile for fulfilling structural design requirements. However, these same design flexibilities render the assessment of composite structural response and durability more complex, prolonging the design and certification process and adding to the cost of the final product. It is difficult to evaluate composite structures because of the complexities in predicting their overall congruity and performance, especially when structural degradation and damage propagation take place. The predictions of damage initiation, damage growth, and propagation to fracture are important in evaluating the load carrying capacity, damage tolerance, safety, and reliability of composite structures. The most effective

* Corresponding author. Fax: +1-216-4333252.

0167-8442/96/$15.00 Copyright © 1996 Elsevier Science B.V. All rights reserved.
PII S0167-8442(96)00023-7

way to obtain this quantification is through integrated computer codes that couple composite mechanics with structural analysis and damage progression models. The COmposite Durability STRuctural ANalysis (CODSTRAN) computer code has been developed for this purpose by integrating and coupling the following disciplines: (i) mechanics of composites, (ii) structural analysis (FEM) and (iii) damage progression tracking. CODSTRAN computer code was used to simulate the damage progression in a variety of fiber composite structures such as: progressive fracture of fiber composite thin shell structures [1–3], fiber composite stiffshed panels [4], Stiflened adhesively bonded composite structures [5], dynamic damage progression of a containment structure hit by an escaping blade [6], damage progression in adhesively bonded fiber composite thin shell structures [7] and [8], damage progression in bolted composite structures [9] and simulation of the Iosipescu shear testing [10].

The objective of the present paper is to demonstrate what can be accomplished by integrating composite mechanics, finite element structural analysis, and tracking of composite failure modes into a stand-alone computer code. The computer code in our case is CODSTRAN. Reference to CODSTRAN throughout this report should not be construed neither as NASA endorsement nor as an advertisement of that computer code.

2. Progressive fracture methodology in codstran

CODSTRAN is an integrated computer code which was developed by coupling three modules: composite mechanics (ICAN [11]), finite element analysis (MHOST [12]) and a damage progression modelling algorithm:

(1) ICAN is a composite mechanics computer code [11] that provides the constituent (fiber and matrix) material properties using an available data bank, and computes the ply properties and the composite properties (effective properties) of the laminate in a hygrothermal environment. The theory of the code is based on the micromechanics of composites and the laminate theory. ICAN has the ability to compute the ply stresses by knowing the stress resultants (force per laminate thickness, where force can

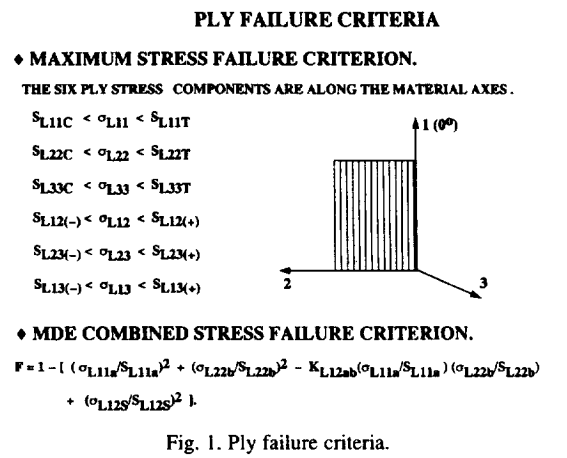

Fig. 1. Ply failure criteria.

be a concentrated load, a bending or a twisting load). In ICAN failure criteria were established (Fig. 1), for the detection of the ply failures as follows: (a) the maximum stress criterion, in which failure occurs when the individual ply stress σ_{Lij} for $i,j = 1,2,3$, exceeds the respective ply strength S_{Lij} for $i,j = 1,2,3$; and (b) the modified distortion energy criterion, in which the combination of the ply stresses is taken into account. In Fig. 1, a and b are referred to the tensile and compressive stresses, respectively. In both criteria the ply stresses are referred to the material axes 1, 2, 3, and the direction of the 0° fibers are along the direction of the material 1-axis. For example a laminate with configuration $(90/0/\pm 75)$ and ply stresses at the top ply (90°) are shown in Fig. 2. In ICAN, the described failure modes of the plies are: failure due to the fiber

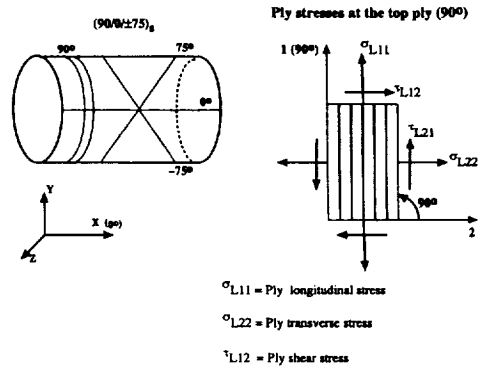

Fig. 2. A typical laminate configuration $(90/0/\pm 75)$ and the ply stresses at the top ply (90°).

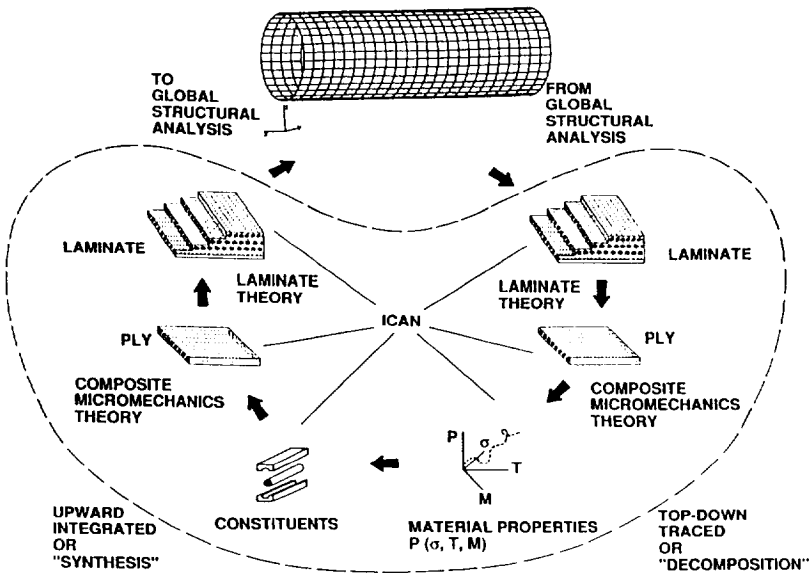

Fig. 3. CODSTRAN progressive fracture simulation cycle.

fracture in tension or in compression; damage due to the matrix fracture in tension or in compression; and damage due to intralaminar and interlaminar shear fracture.

(2) MHOST is a finite element computer code [12] for the solution of structural analysis problems. The code has the capability to perform linear or nonlinear static and dynamic analysis. MHOST has a library with a variety of elements and for the present work the four node shell element was used. By supplying the boundary conditions, the desire type of analysis, the applied loads and the laminate properties (using ICAN) MHOST performs the structural analysis. In addition MHOST provides the computed stress resultants to the ICAN code; and then ICAN computes the developed ply stresses for each ply and checks for ply failure.

(3) A module that keeps track the failure modes and communicate these modes to ICAN in order to degrade the properties associated with the respected failure modes.

An integrated schematic of the CODSTRAN simulation cycle is shown in Fig. 3. In this figure, from the left side along the clockwise direction the material properties of the constituents (fiber and matrix) are provided by ICAN's data bank, next the ply properties are computed by using the micromechanics theory, and the laminate properties are computed using the laminate theory. These properties in conjunction with the finite element mesh, the loads and the boundary conditions are incorporated into MHOST. MHOST performs the structural analysis and provides the computed stress resultants in ICAN (in the right side of Fig. 3), where ICAN proceeds to compute the ply stresses using the laminate theory and checks for ply failure.

The nonlinear structural analysis in MHOST code is performed in conjunction with an incremental load algorithm. The load is increased in small increments

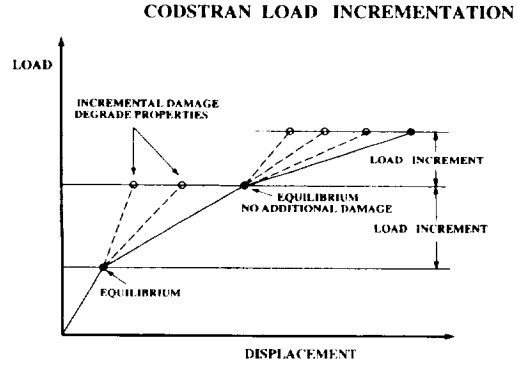

Fig. 4. CODSTRAN load increment.

(equilibrium positions). Within each equilibrium position a number of iterations are performed for damage growth and accompanying internal structural response to sustain the applied load, Fig. 4. In each iteration, the structure is checked for ply failure. If damages are detected in the structure, the model is automatically updated with a new finite element mesh and new laminate properties, and a new finite element analysis is performed; the above iterations continue until no further damage occurs (equilibrium position). After that, the load is increased, and the above procedure is repeated until the final failure of the structure. Following the above procedure, the damage progression, fracture and collapse of the structure is monitored.

3. Geometry, loads, materials and the FE model of the thin shell

The geometry of the fiber composite shell is a thin cylinder. The thin cylinder has inner diameter of 305 mm (12 in.) and length of 760 mm (30 in.). The boundary conditions are one end fixed supported and the other free. The corresponding graphite fibers (AS-4) and epoxy matrix (HMES) properties of the fiber composite thin shell were obtained from a data bank of composite constituent material properties resident in CODSTRAN and are given in Tables 1 and 2, respectively. The AS4/HMES ply strengths computed by ICAN code are given in Table 3. The fiber composite thin shell consists of eight 0.136 mm (0.00535 in.) plies resulting in a composite shell thickness of 1,088 mm (0.0428 in.). The laminate configuration is $(90/0/\pm 75)$, with the 90° plies in the hoop (or circumferential) direction and the 0° plies in the axial direction. Fiber orientations in the $\pm 75°$ is shown in Fig. 2. The fiber volume ratio is 60% and the void volume ratio is 2% of the total volume of the structure. The residual stresses is been taken into account due to the processing. The cure temperature was 177°C (350°F) and the pressurization/use temperature is 21°C (70°F). The moisture content was zero. The closed-end cylindrical pressure vessel is simulated by applying a uniformly

Table 1
AS-4 graphite fiber properties

Number of fibers per end = 10000
Fiber diameter = 0.00762 mm (0.3E-3 in)
Fiber density = 4.04×E−7 kg/m^3 (0.063 lb/in^3)
Longitudinal normal modulus = 227 GPa (32.9×E+6 psi)
Transverse normal modulus = 13.7 GPa (1.99×E+6 psi)
Poisson's ratio (ν_{12}) = 0.2
Poisson's ratio (ν_{23}) = 0.25
Shear modulus (G_{12}) = 13.8 GPa (2×E+6 psi)
Shear modulus (G_{23}) = 6.9 GPa (1×E+6 psi)
Longitudinal thermal expansion coefficient = 1×E−6/°C (−0.55×E−6/°F)
Transverse thermal expansion coefficient = 1×E−6/°C (−0.56×E−6/°F)
Longitudinal heat conductivity = 43.4 J m/h/m^2/°C (580 BTU-in/h/in^2/°F)
Transverse heat conductivity = 4.34 J m/h/m^2/°C (58 BTU-in/h/in^2/°F)
Heat capacity = 712 J/kg/°C (0.17 BTU/lb/°F)
Tensile strength = 3723 MPa (540 psi)
Compressive strength = 3351 MPa (486 psi)

Table 2
HMHS epoxy matrix properties

Matrix density = 3.4×E−7 kg/m^3 (0.0457 lb/in.^{3})
Normal modulus = 4.27 GPa (629 psi)
Poisson's ratio = 0.34
Coefficient of thermal expansion = 0.72/°C (0.4×E−4/°F)
Heat conductivity = 1.25 BTU-in./h/in.^{2}/°F
Heat capacity = 0.25 BTU/lb/°F
Tensile strength = 84.8 MPa (12.3 psi)
Compressive strength = 423 MPa (61.3 psi)
Shear strength = 148 MPa (21.4 psi)
Allowable tensile strain = 0.02
Allowable compressive strain = 0.05
Allowable shear strain = 0.04
Allowable torsional strain = 0.04
Void conductivity = 16.8 J m/h/m^2/°C (0.225 BTU-in./h/in.^{2}/°F)
Glass transition temperature = 216°C (420 °F)

Table 3
AS-4/RMHS ply strengths

S_{L11T} = 1930.30 MPa (280 psi)
S_{L11C} = 1475.85 MPa (210 psi)
S_{L22T} = 91.38 Mpa (13 psi)
S_{L22C} = 228.27 MPa (33 psi)
S_{L12} = 65.57 MPa (9.5 psi)
S_{L23} = 59.98 MPa (8.7 psi)

Where 1, 2, 3 are the material axes of the ply. The direction of the fibers are parallel to 1-axis. T is for tension and C is for compression.

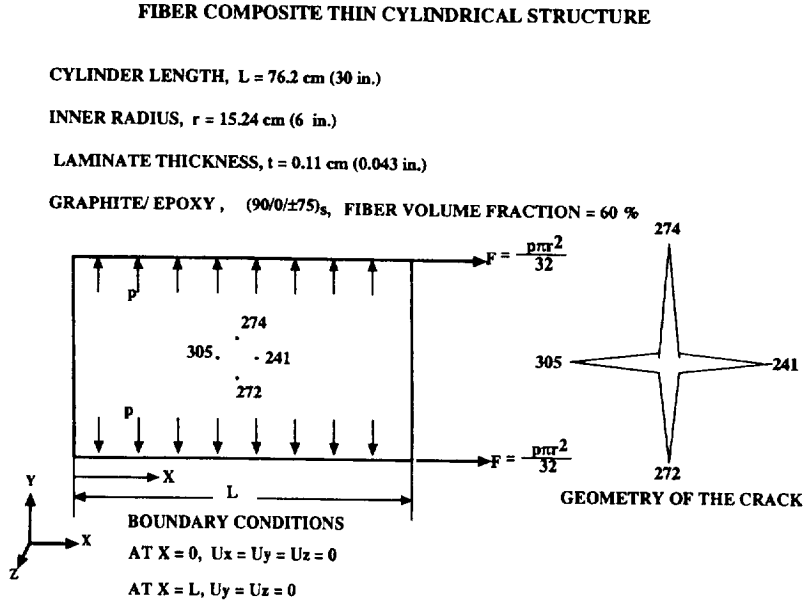

Fig. 5. Applied loads and boundary conditions of the thin shell structures.

distributed axial tension such that the generalized axial stresses in the shell wall were half of those developed in the hoop direction, Fig. 5. The shell is subjected to a monotonically increasing internal pressure until it burst. Shells with defect and defect free are examined. The defective shell has a through-the-thickness defect at a node located at the half length of the shell. After the load is applied in the defective shell, a crack is formed at the location of the defective node as shown in Fig. 5. The geometry of the formed crack consists of a 95 mm (3.75 in.) long thin axial slit that is superimposed on a 60 mm (2.36 in.) long circumferential slit. Each finite element model contained 544 nodes and 512 uniformly sized rectangular elements, Fig. 6. Damage initiation, growth, fracture progression, and global structural

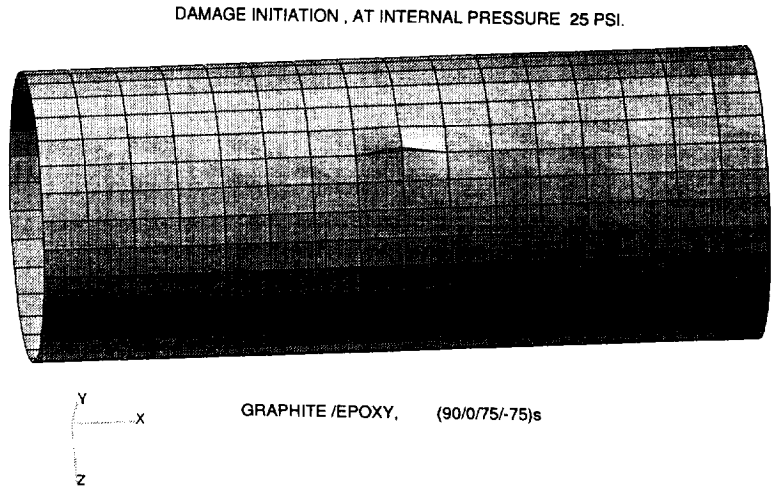

Fig. 6. Finite element mesh.

fracture stages were investigated. Computed results are presented up to global fracture for defect-free shells and shells with through-the-thickness defects.

4. Results and discussion

(1) Fiber composite $(90/0/\pm 75)$, free defects thin shells. The damage of the thin shell structure is plotted versus the internal pressure in Fig. 7.1. Damage is defined as the ratio of the volume of the damaged plies divided by the total volume of the plies. The depicted points of Fig. 7.1 are equilibrium points that were discussed in the previous chapter in CODSTRAN Methodology. Damage initiation occurred at pressure of 1.06 MPa (153 psi) with matrix cracking at the outermost ply 2 (0°). The damage progressed with shear failure at the ply 3 (75°) and matrix cracking at the plies 7 (0°) and 8 (90°). Further, the damage progressed and matrix cracking occurred at the outermost ply 1 (90°), and at the 5 (−75°) and 6 (75°). After the initial matrix degradation stage the pressure was increased without activating additional damage modes. The thin shell burst

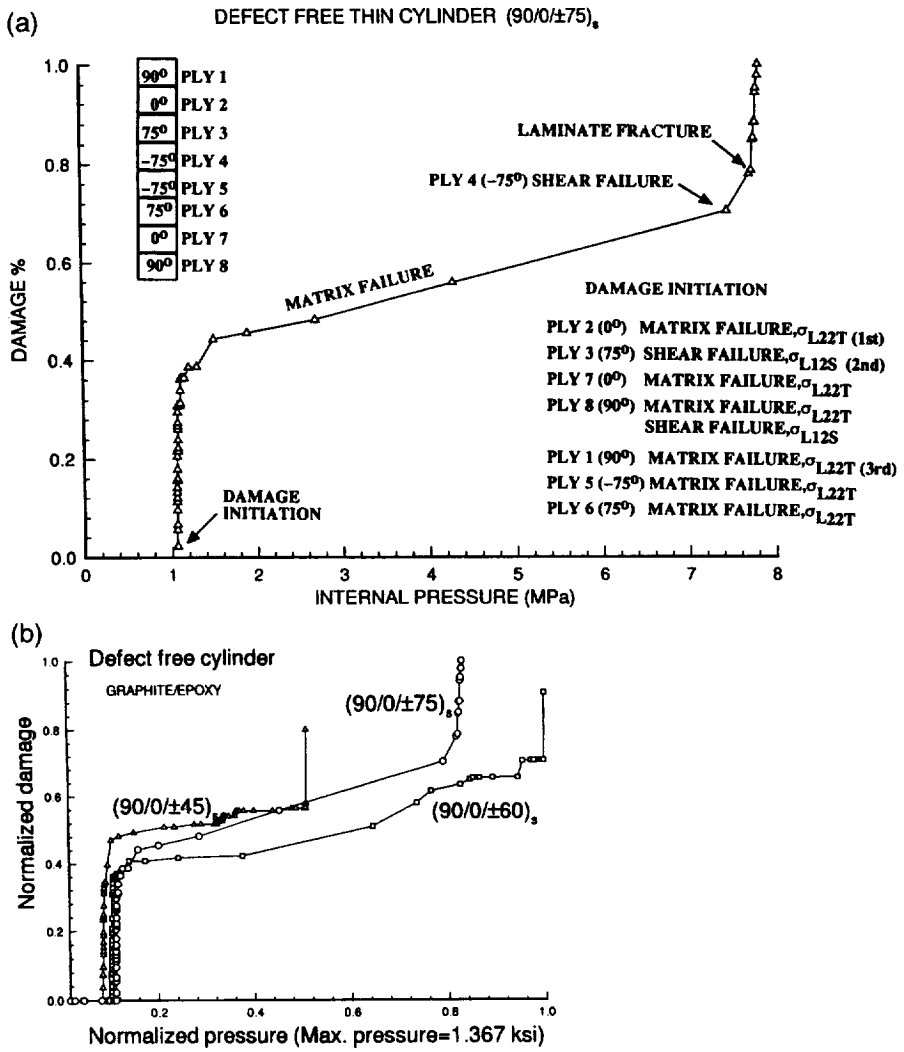

Fig. 7. (1) Damage versus pressure in defect-free thin shell. (2) effect of the laminate configuration, on the damage of the defect-free thin shells.

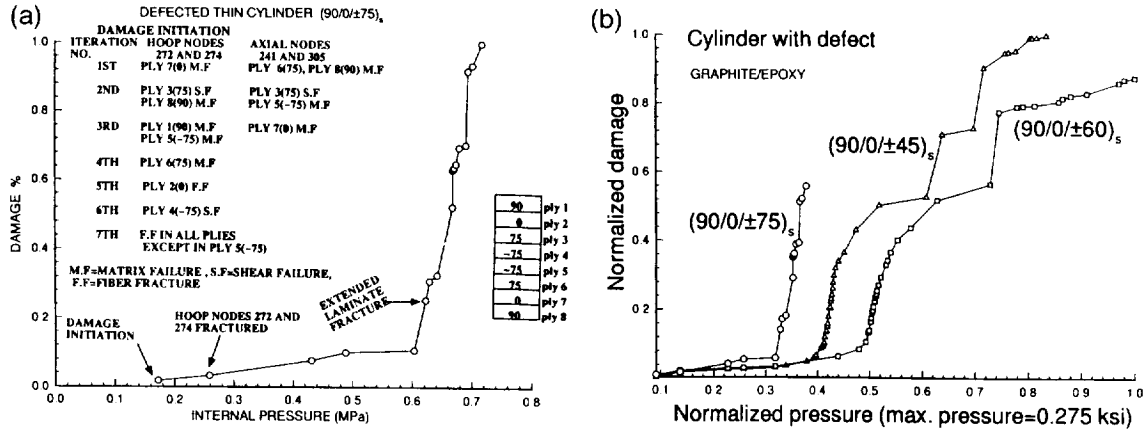

Fig. 8. (1) Damage versus pressure in defective thin shell. (2) Effect of the laminate configuration, on the damage of the defected thin shells.

when ply 2, the outermost 0° axial ply experienced fiber fractures that caused rapid damage propagation to the other plies and structural fracture. The structural fracture was initiated by the tensile failure of axial fibers. The simulated burst pressure was 7.83 MPa (1.14 psi).

The damage progression of the $(90/0/\pm 75)$ laminate compared with the $(90/0/\pm 45)$, and $(90/0/\pm 60)$, layup configurations in Fig. 7.2. In the case of the $(90/0/\pm 45)$, laminate, damage initiation occurred at 0.8 MPa (116 psi) with matrix cracking in the first ply (0°) followed by the 45° ply immediately adjacent to it, then the innermost (0°) ply and the 90° ply on the interior surface. After damage initiation, all plies gradually sustained matrix cracking as the pressure was increased to 0.84 MPa (121 psi). After this damage accumulation stage the pressure was significantly increased without activating additional damage modes. The thin shell burst when the 90 hoop plies experience fiber fractures at 4.8 MPa (696 psi). In the case of the $(90/0/\pm 60)$, laminate, initial damage occurred at 0.97 MPa (140 psi) with matrix cracking at the 2nd ply (0) followed by the 3rd ply (60) then by the 7th ply (0) and finally by the 8th ply (90). After damage initiation, all plies gradually sustained matrix cracking as the pressure

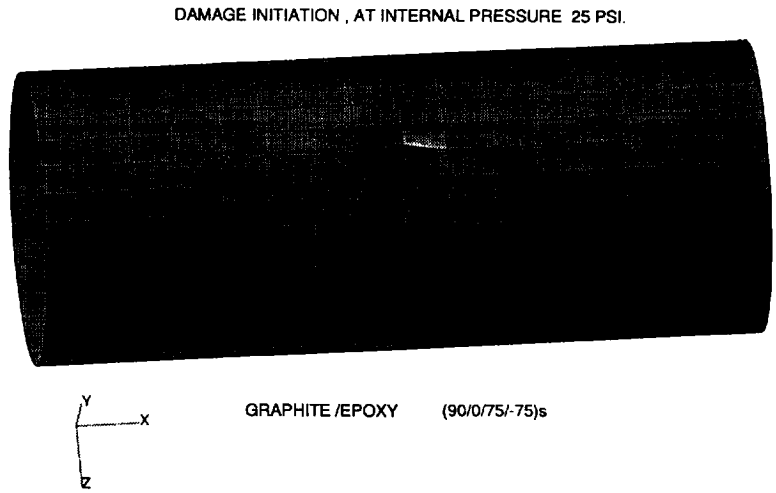

Fig. 9. Damage initiation at 0.17 MPa (25 psi).

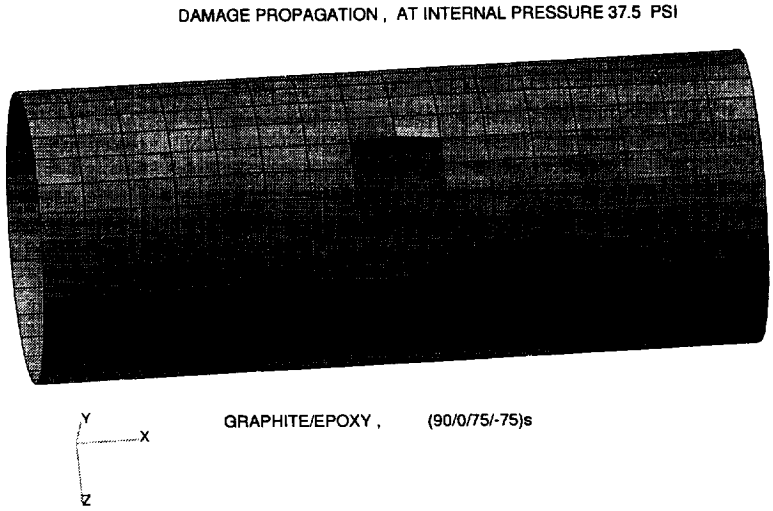

Fig. 10. Damage progression at 0.26 MPa (37.5 psi).

was retained virtually constant. After this damage accumulation stage, the pressure was significantly increased without activating additional damage modes. The thin shell burst when the outermost 90° hoop plies experienced fiber fractures at 9.42 MPa (1366 psi).

(2) $(90/0/\pm 75)$, fiber composite defective thin shells. The damage versus the internal pressure is shown in Fig. 8.1. The damage initiated at internal pressure of 0.172 MPa (25 psi.) with matrix fracture along the hoop direction nodes 272 and 274 in the 7th (0°) ply and along the axial direction nodes 241 and 305 in the 6th (75°) and 8th (90°) plies. The damage progressed continuously with shear failure at the 3rd (75°) ply in both hoop and axial nodes, and with matrix failure at the 8th (90°) ply at the hoop and at the 5th ($-75°$) ply, at the axial node. The damage of the plies continued with relatively small increases in pressure in the hoop direction until fiber fracture occurred at all plies except of the 5th ($-75°$).

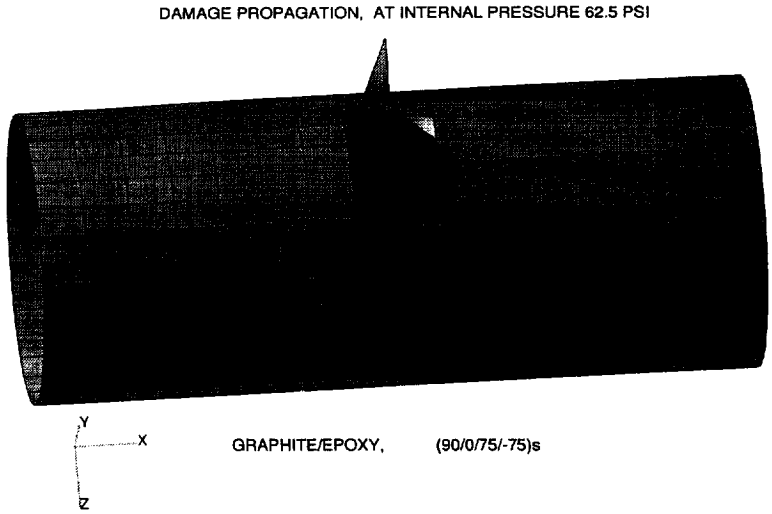

Fig. 11. Damage progression at 0.43 MPa (62.5 psi).

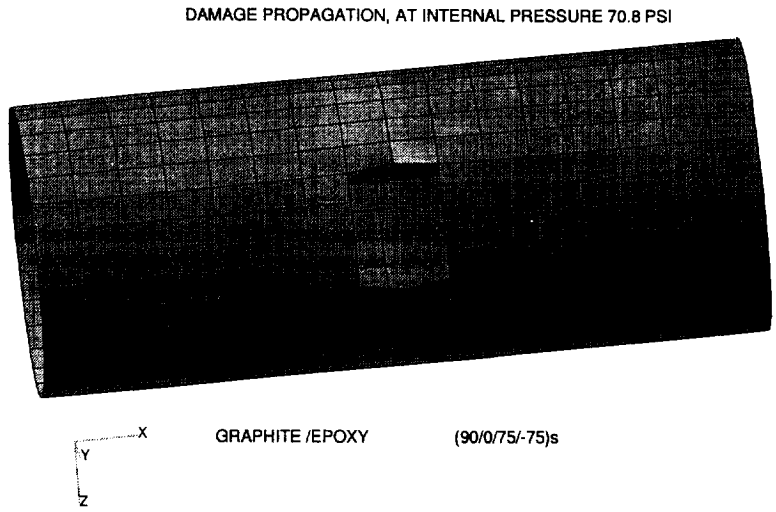

Fig. 12. Damage progression at 0.49 MPa (70.8 psi).

Increasing the load further, the damage of the shell progressed steadily until it reached the value of 0.62 MPa (90 psi) where the fracture growth became unstable, increased rapidly, and structural fracture occurred at burst pressure equal to 0.717 MPa (104 psi).

The damage progression of the $(90/0/\pm 75)$ laminate compared with the $(90/0/\pm 45)$ and $(90/0/\pm 60)$ layup configurations as shown in Fig. 8.2. In the case of $(90/0/\pm 45)$ laminate, the damage initiation started at pressure 0.175 MPa (25 psi). The damage growth localized adjacent to the defect until a 0.74 MPa (108 psi) pressure reached. Damage propagation by fiber fractures concentrated near the defect. The thin shell burst at pressure equal to 1.58 MPa (230 psi). In the case of $(90/0/\pm 60)$ laminate, damage initiation started at pressure 0.17 MPa (25 psi) by matrix cracking adjacent to the defect at the 8th ply (90°) at the circumferential slit tips and by the 7th ply (0°) at the axial slit tips. Damage

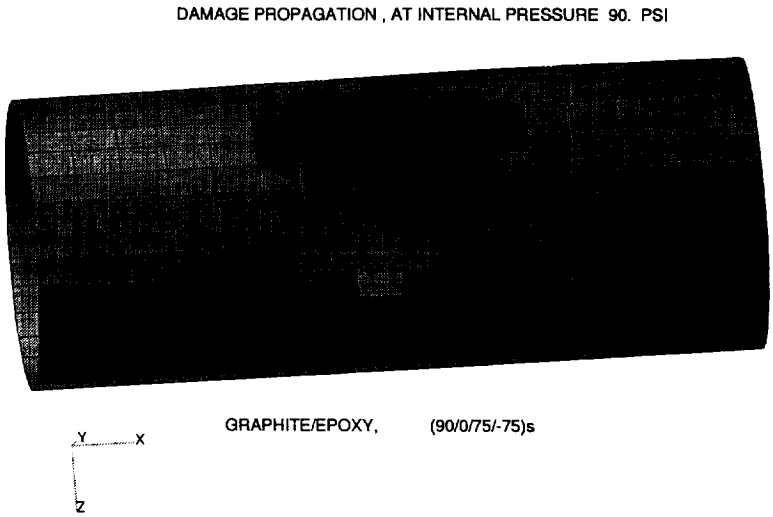

Fig. 13. Damage progression at 0.62 MPa (90.0 psi).

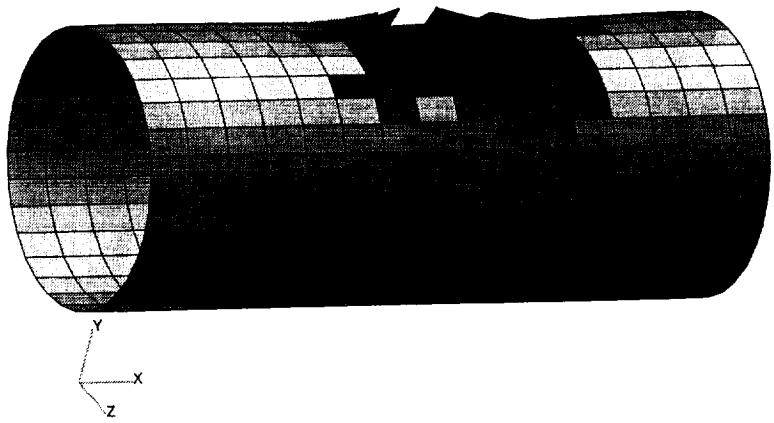

Fig. 14. Collapse of the defective shell at 0.71 MPa (104 psi).

growth remained localized adjacent to the defect as the pressure was increased to 0.91 MPa (132 psi). The thin shell burst at 1.9 MPa (275 psi).

Regarding the comparison of the direction of the damage progression: the damage growth of the $(90/0/\pm 45)$ laminate was mainly in the axial direction of the shell. The damage growth of the $(90/0/\pm 75)$ laminate was mainly in the circumferential direction of the shell. Finally, the direction for the damage growth for the $(90/0/\pm 60)$ laminate was both in the circumferential as well as in the axial direction.

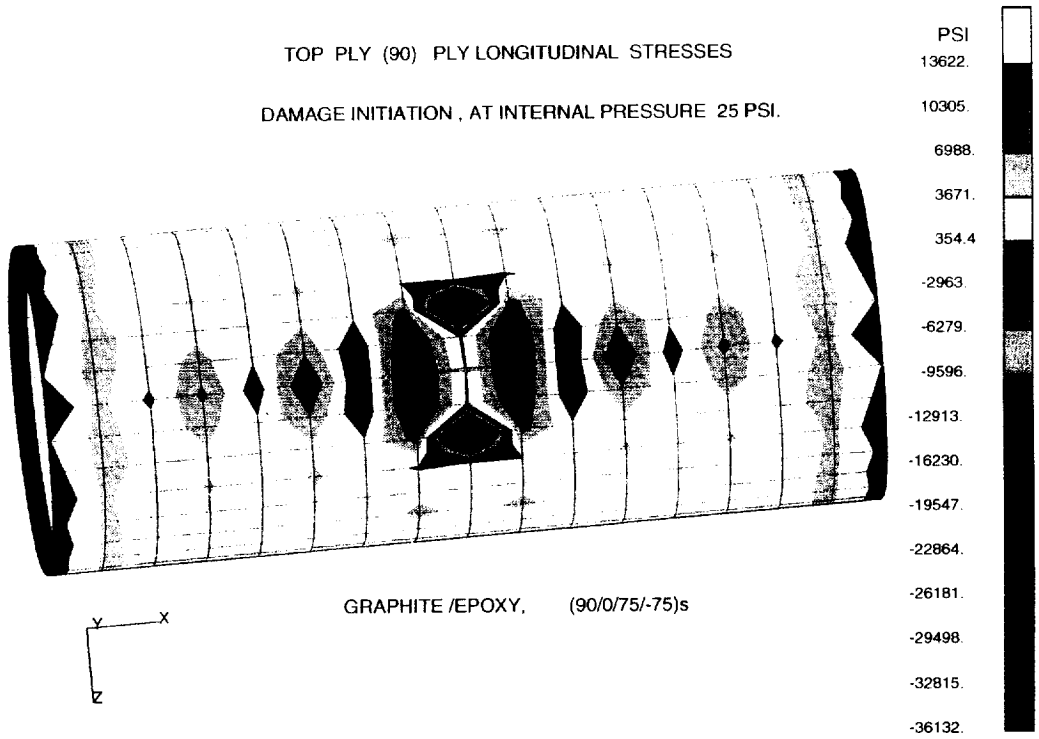

Fig. 15. At the top ply (90°), ply longitudinal stresses at 0.17 MPa (25 psi).

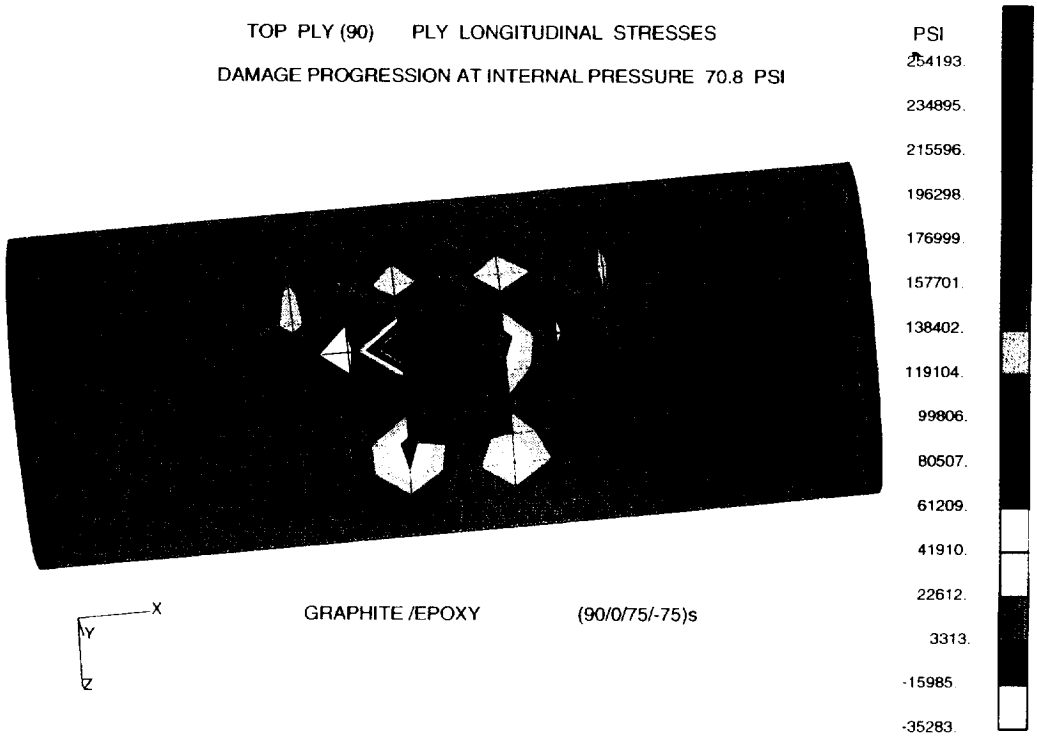

Fig. 16. At the top ply (90°), ply longitudinal stresses at 0.49 MPa (70.8 psi).

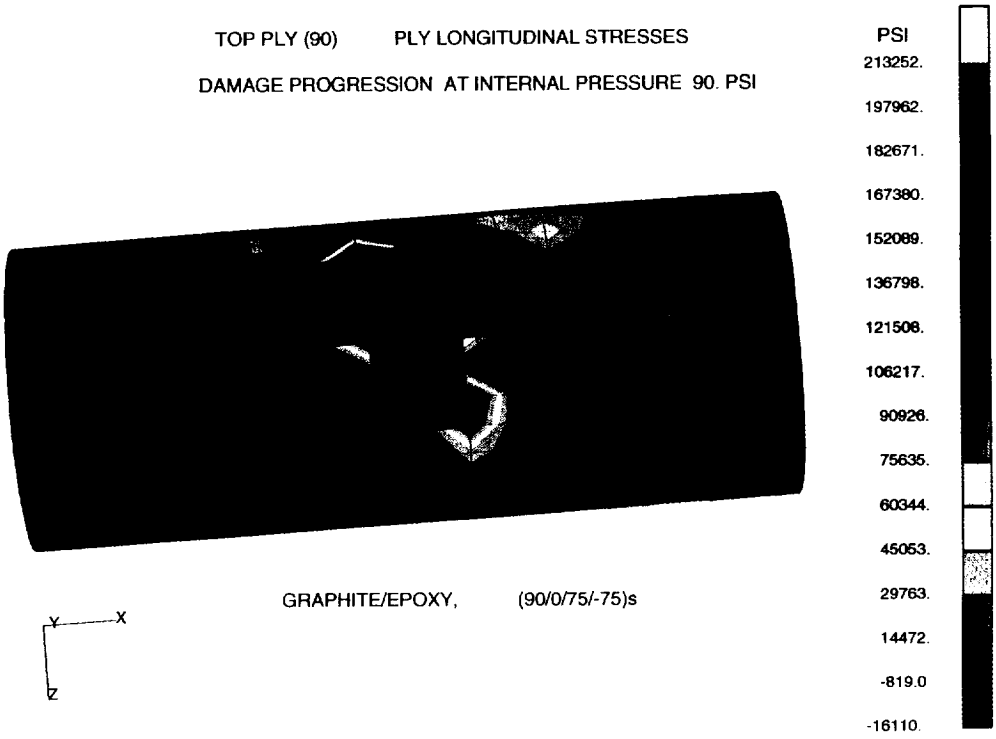

Fig. 17. At the top ply (90°), ply longitudinal stresses at 0.62 MPa (90 psi).

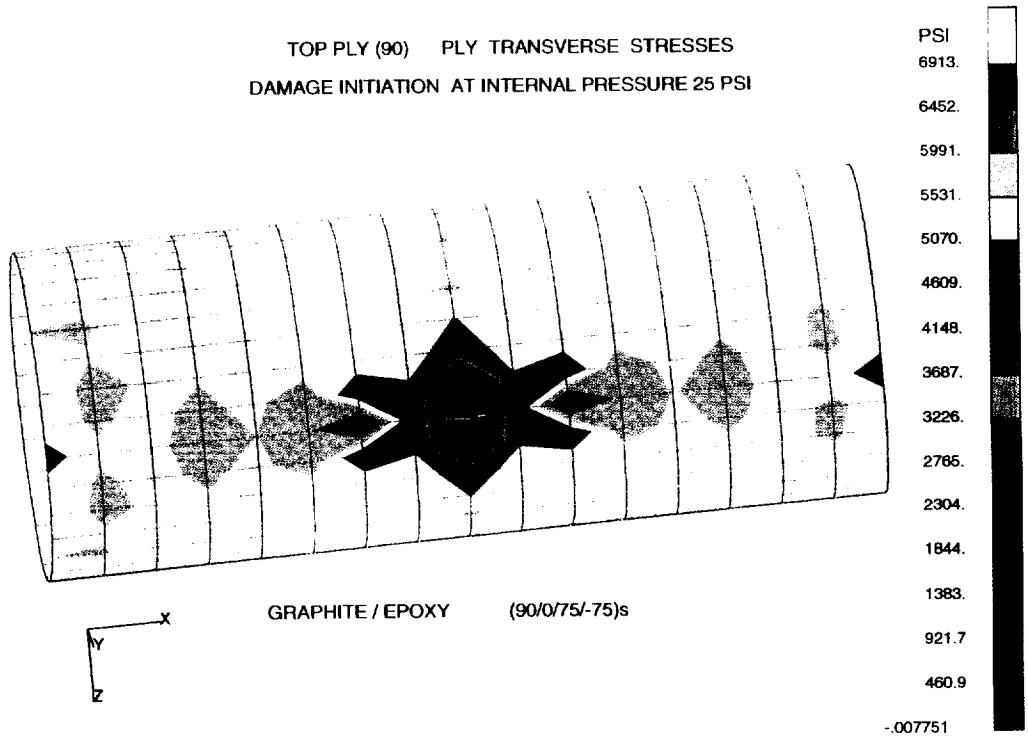

Fig. 18. At the top ply (90°), ply transverse stresses at 0.17 MPa (25 psi).

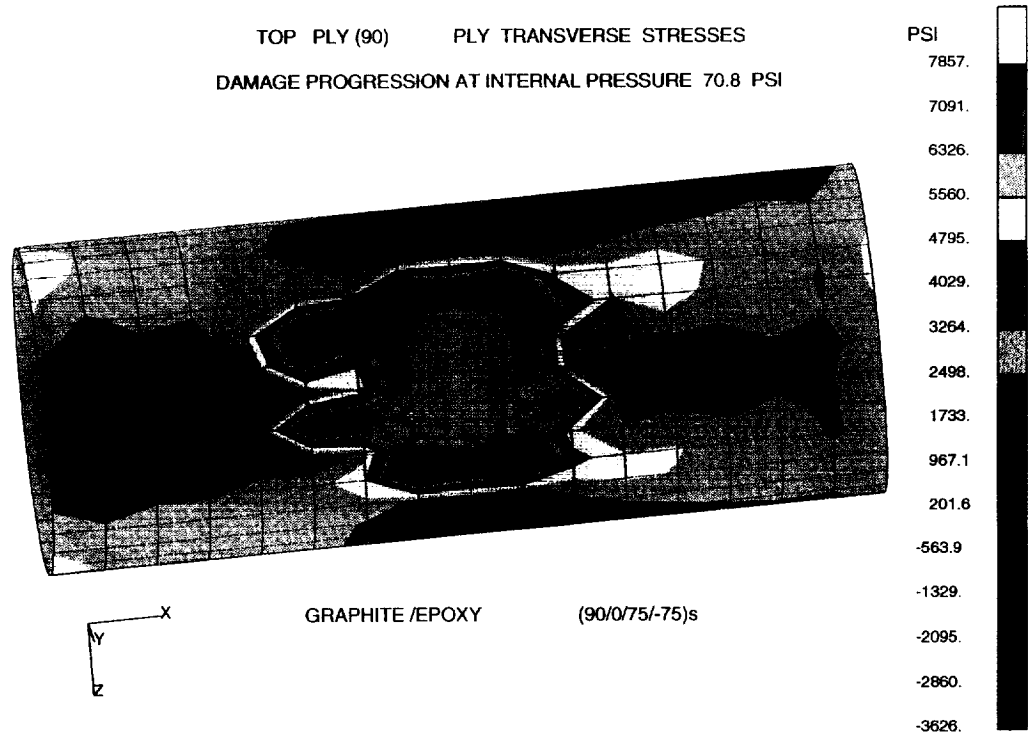

Fig. 19. At the top ply (90°), ply transverse stresses at 0.49 MPa (70.8 psi).

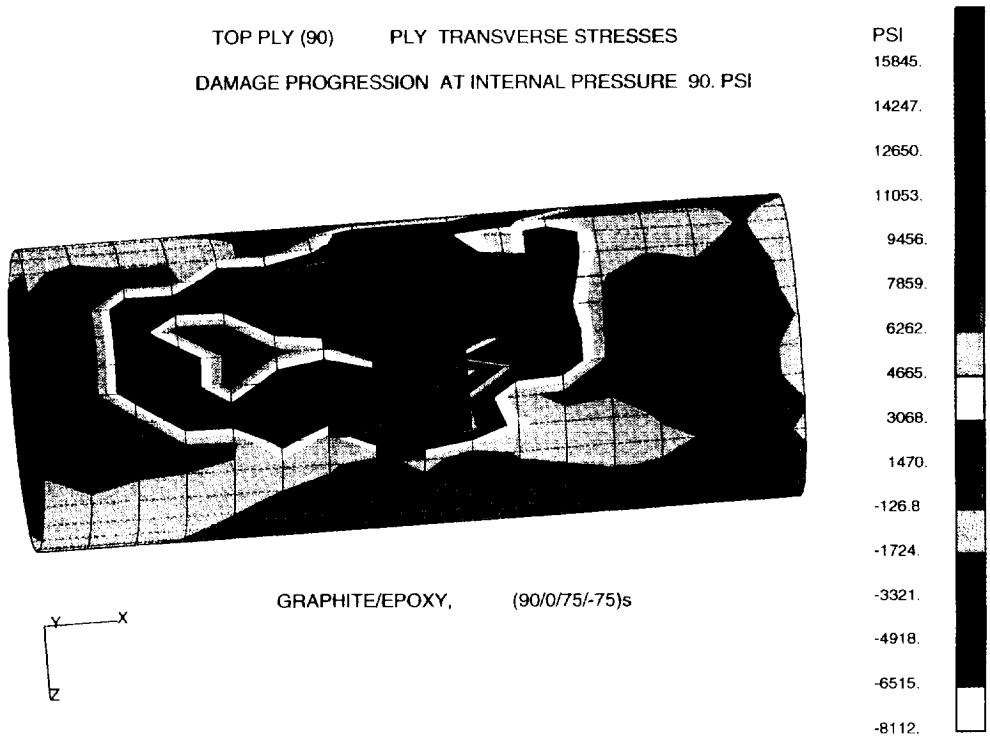

Fig. 20. At the top ply (90°), ply transverse stresses at 0.62 MPa (90 psi).

The fracture progression of the $(90/0/\pm 75)$ thin shell structure is depicted in Figs. 9–14, for different load increments. At the top ply (90°), the ply longitudinal stresses (in the hoop direction) are plotted in Figs. 15–17; and the ply transverse stresses (in the axial direction) are plotted in Figs. 18–20 for different load increments. At the damage initiation stage high ply stresses were developed at the edges of the crack, and when the fracture progressed the distribution of the ply stresses around the fractured area changed and decreased.

5. Summary

In this investigation, the simulation of the structural and damage progression response of a $(90/0/\pm 75)$, composite thin shell structure was examined. The damage progression of the $(90/0/\pm 75)$ laminate was compared with the $(90/0/\pm\theta)$, (for $\theta = 45$ and 60) layup configurations. The significant results are as follows:

(1) For the case of the defect free $(90/0/\pm 75)$ thin shell structure damage initiation started at internal pressure 0.14% of the burst pressure 7.83 MPa (1.1 psi) with matrix cracking at the outermost ply 2 (0°) and followed by the same type of failure at the plies 3 (75°), 7 (0°) and 8 (90°). The damage progressed and when fiber fractured occurred at the outermost ply 2 (0°) rapid fracture initiated and collapse of the structure occurred at 0.717 MPa (0.104 psi).

(2) For the case of the defected $(90/0/\pm 75)$ thin shell structure, the damage initiation started at internal pressure of 0.24% of the burst pressure 0.717 MPa (0.104 psi), with matrix cracking at the plies near the nodes of the crack tips (hoop and the axial directions nodes). Increasing the applied pressure, the fiber fracture progressed in the hoop direction at a faster rate than in the axial direction, until the collapse of the structure.

(3) Comparing the defected with the defect free thin shell structure, it was observed that damage initiation started at 0.16% of the defect free thin shell

pressure 1.06 MPa (0.153 psi), while burst pressure occurred at 0.991% of the defect free thin shell pressure 7.83 MPa (1.13 psi).

(4) The direction of damage growth for the $(90/0/\pm 75)$ laminate was mainly in the circumferential direction of the defected shell. This laminate was the least damage tolerant of the two compared defective shells with $(90/0/\pm 45)$ and $(90/0/\pm 60)$ layup configurations.

(5) The direction of damage growth for the $(90/0/\pm 45)$ laminate was mainly in the axial direction of the defective shell, had significant damage tolerance and sustained the maximum amount of damage prior to bursting.

(6) The direction of damage growth for the $(90/0/\pm 60)$ laminate was both in the circumferential as well as in the axial direction of the defected shell. This laminate was able to sustain the highest burst pressure. However, the amount of damage sustained was lower than that corresponding to the $(90/0/\pm 45)$ laminate.

References

[1] P.K. Gotsis, C.C. Chamis and L. Minnetyan, Defect tolerance of pressurized fiber composite shell structures, in: *Proc. of the 41st Int. SAMPE Symp. and Exhibition, Anaheim, CA*, March 25–28, 1996, Vol. 41 (450–461, 1996).

[2] P.K. Gotsis, C.C. Chamis and L. Minnetyan, Progressive fracture of fiber composite thin shell structures under internal pressure and axial loads, *NASA TM* 107234 (1996) in preparation.

[3] C.C. Chamis, P.K. Gotsis and L. Minnetyan, Damage tolerance of composite pressurized shells, in: *Proc. of the 37th AIAA / ASME / ASCE / AHS / ASC Struct., Struct. Dynam., and Mater. Conf., Salt Lake City, UT*, April 15–17, 1996, Part 4 (2112–2121, 1996).

[4] P.K. Gotsis, C.C. Chamis and L. Minnetyan, Progressive fracture of fiber composite build-up structures, *J. Reinforced Plastic Composites* (1996) submitted for publication; *NASA TM* 107231 (1996) submitted for publication.

[5] P.K. Gotsis, C.C. Chamis and L. Minnetyan, Effect of combined loads in the durability of a stiffened adhesively bonded composite structure, in: *Proc. of the 36th AIAA / ASME / ASCE / ABS / ASC Struct., Struct. Dynam., and Mater. Conf., New Orleans, LA*, April 10–13, 1995, Part 2 (1083–1092, 1995).

[6] P.K. Gotsis, C.C. Chamis and L. Minnetyan, Progressive fracture of blade containment composite structures, in: *Proc. of the 11th DOD / NASA / FAA Conf. on Fibrous Composites in Struct. Design, Fort Worth, TX*, August 26–29, 1996 (submitted for publication).

[7] L. Minnetyan and P.K. Gotsis, Progressive fracture in adhesively bonded concentric cylinders, in: *Proc. of the 40th SAMPE Symp. and Exhibition, Anaheim, CA*, May 8–11, 1995, Vol. 40, Book 1 (849–860, 1995).

[8] C.C. Chamis, P.K. Gotsis and L. Minnetyan, Progressive damage and fracture of adhesively bonded fiber composite pipe joints, in: *Proc. of the Conf. and Exhibitions, 1996: Symp. on Composite Mater., Design and Anal., Houston, TX*, Jan. 29–Feb. 2, 1996, Book V (401–408, 1996).

[9] C.C. Chamis, P.K. Gotsis and L. Minnetyan, Damage progression in bolted composite structures, in: *Proc. of the USAF Struct. Integrity Program Conf., San Antonio, TX*, Nov. 28–30, 1995, in press.

[10] L. Minnetyan, D. Huang, C.C. Chamis and P.K. Gotsis, Progressive fracture of composite subjected to Iosipescu shear testing, in: *Proc. of the ASTM 13th Symp. on Composite Mater.: Testing and Design, Orlando, FL*, May 20–21, 1996.

[11] P.L.N. Murthy and C.C. Chamis, *ICAN (Integrated Composite ANalyzer computer code) Users Manual*, NASA TP 2515, 1986.

[12] S. Nakazawa, J.B. Dias and M.S. Spiegel, *MHOST Users Manual*, Prepared for NASA Lewis Research Center by MARC Analysis Research Corp., April 1987.

THEORETICAL AND APPLIED FRACTURE MECHANICS

Aims and Scope
Mechanics and Physics of Fracture

The "Mechanics and Physics of Fracture" section encourages publication of original research on material damage leading to crack growth and/or fatigue. Materials treated include metal alloys, polymers, composites, rocks, ceramics, etc. The material damage process is complex because it involves the combined effect of loading, size and geometry, temperature and environment. Formulation may involve the dissipation of energy in various forms and the identification of microscopic entities and their interactions with macroscopic variables. The advent of the modern computer, however, has offered added capability for analyzing the stresses and/or strains and failure modes. The construction and verification of quantitative theories can be more readily carried out. Encouraged in particular are contributions related to predictions of material damage behavior based on microscopic and/or macroscopic models.

Aims and Scope
Fracture Mechanics Technology

The "Fracture Mechanics Technology" section emphasizes material characterization techniques and translation of specimen data to design. Contributions shall cover the application of fracture mechanics to hydro and electric machineries, off-shore oil exploration equipments, pipelines and pressure vessels, nuclear reactor components, air, land and sea vehicles, and many others. Among the areas to be emphasized are:

- Case Histories
- Material Selection and Structure Design
- Sample Calculations of Practical Design Problems
- Material Characterization Procedures
- Fatigue Crack Growth and Corrosion
- Nondestructive Testing and Inspection
- Code Requirements and Standards
- Structural Failure and Aging
- Failure Prevention Methodologies
- Maintenance and Repair
- Product Liability and Technical Insurance

Subscription Information

THEORETICAL AND APPLIED FRACTURE MECHANICS (ISSN 0167-8442). For 1996 volumes 25 and 26 are scheduled for publication.
Subscription prices are available upon request from the publisher. Subscriptions are accepted on a prepaid basis only and are entered on a calendar year basis. Issues are sent by surface mail except to the following countries where air delivery via SAL mail is ensured: Argentina, Australia, Brazil, Canada, China, Hong Kong, India, Israel, Japan, Malaysia, Mexico, New Zealand, Pakistan, Singapore, South Africa, South Korea, Taiwan, Thailand, USA. For all other countries airmail rates are available upon request.

Claims for missing must be made within six months of our publication (mailing) date.

Please address all your requests regarding orders and subsciption queries to: Elsevier Science B.V., Journals Department, P.O. Box 211, 1000 AE Amsterdam, The Netherlands. Tel.: 31-20-4853642, FAX: 31-20-4853598.

Information for Contributors

Manuscripts in English should be submitted in triplicate to the Editor-in-Chief or communicated via a member of the Board of Editors who is most closely associated with the content of the work. In the latter case, one copy of the manuscript should be sent to the office of the Editor-in-Chief.

Upon acceptance of an article, the author(s) will be asked to transfer copyright of the article to the publisher. This transfer will ensure the widest possible dissemination of information.

There are no page charges. Cost for alterations in proofs other than printer's errors will, however, be charged to the authors.

Fifty reprints of each paper will be provided free of charge. Additional reprints can be ordered at cost.

The language of the manuscript should be in English. Manuscripts submitted in other languages may be considered at the discretion of the Board of Editors.

Manuscripts should be typed double spaced on one side of the page only with wide margins. The first page of the manuscript should contain: a title, name(s) of author(s), affiliation(s), and a short abstract. The author to whom the proofs should be sent must be indicated with her/his full postal address, telephone number, fax number and/or e-mail address. One to four classification codes (PACS and/or MSC) and up to six keywords of the author's choice should be given below the abstract. The PACS'96 and MSC'91 lists are available on the Elsevier web server: http://www.elsevier.nl

All mathematical symbols which are not typewritten should be specified and listed separately. Unusual symbols or notations should be identified in the margins. Awkward mathematical notations which require special typesetting procedures must be avoided. The numbers identifying displayed mathematical expressions should be placed in parentheses. The use of metric units of the SI (Système Internationale) form is obligatory.

Illustrations are to be restricted to the minimum necessary. Originally drawn figures and glossy prints of photographs should be provided in a form suitable for photographic reproduction and reduction. Each figure should have a number and a caption; the captions should be collected on a separate sheet.

References to published literature should be quoted in the text in square brackets and grouped together at the end of the paper in numerical order. Journal titles should be abbreviated in the style of the 4th edition of the World List of Scientific Periodicals, and references should be arranged as

[1] L.F. Gillemot, Criterion of crack initiation and spreading, *J. Eng. Fract. Mech. 8*, 239–253 (1976).

for journal articles and

[2] N.I. Muskhelishvili, *Some Basic Problems of the Mathematical Theory of Elasticity*, Second English ed. (Noordhoff, Groningen, Netherlands, 1963).

ELSEVIER SCIENCE

prefers the submission of electronic manuscripts

Electronic manuscripts have the advantage that there is no need for the rekeying of text, thereby avoiding the possibility of introducing errors and resulting in reliable and fast delivery of proofs.

The preferred storage medium is a 5.25 or 3.5 inch disk in MS-DOS format, although other systems are welcome, e.g. Macintosh.

After **final acceptance,** your disk plus one final, printed and exactly matching version (as a printout) should be submitted together to the accepting editor. **It is important that the file on disk and the printout are identical.** Both will then be forwarded by the editor to Elsevier.

Please follow the general instructions on style/arrangement and, in particular, the reference style of this journal as given in "Instructions to Authors."

Please label the disk with your name, the software & hardware used and the name of the file to be processed.

THEORETICAL AND APPLIED FRACTURE MECHANICS

❒ Please send me a free sample copy

❒ Please send me subscription information

❒ Please send me Instructions to Authors

Name _____

Address _____

_____

_____

ELSEVIER SCIENCE B.V.

Send this coupon or a photocopy to:

ELSEVIER SCIENCE B.V
Attn: Engineering and Technology Department
P.O. Box 1991, 100 BZ Amsterdam, The Netherlands